

PROBLEM SHEET 12

Open Quantum Systems WS18-19

Iyán Méndez Veiga
 iyan.mendez-veiga@uni-ulm.de

Code available here: https://github.com/iyanmv/OQS_ws18-19.

Exercise 26

a) Simulation of a two-site closed system with energy difference $\Delta\Omega = \Omega_1 - \Omega_2 = 0$ and electronic coupling $J = 100$. Perfect coherent energy transfer is observed since there is no interaction with the thermal bath. See Figure 1. Values are plotted from $t = 0$ to $t = 0.1$ so it is possible to observe the fast oscillations.

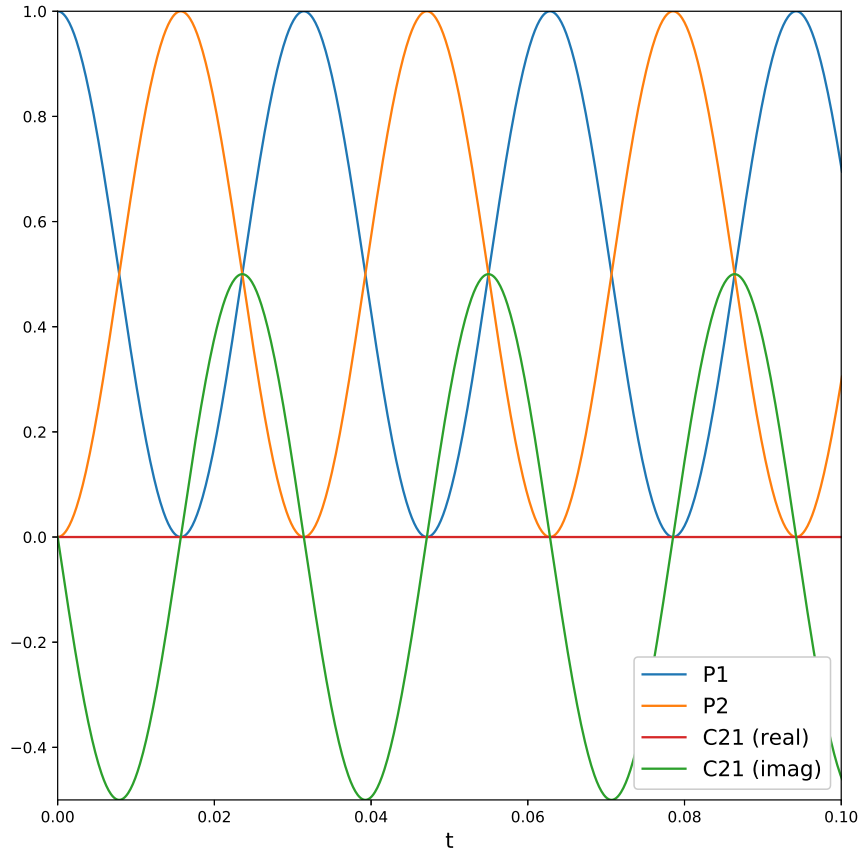


Figure 1: Obtained populations $P_1(t) = \langle 1 | \rho_s(t) | 1 \rangle$ and $P_2(t) = \langle 2 | \rho_s(t) | 2 \rangle$, and inter-site coherence $C_{21}(t) = \langle 2 | \rho_s(t) | 1 \rangle$, using Runge-Kutta method from $t = 0$ to $t = 0.1$.

b) Same parameters as before but now with each site coupled to an independent thermal bath modelled with quantum harmonic oscillators for temperature $(k_B T / \hbar) = 100$. An Ohmic spectral density

$$\mathcal{T}_k(\omega) = \frac{2\lambda_k}{\pi} \frac{\omega \gamma_k}{\omega^2 + \gamma_k^2} \quad (1)$$

was used with $\lambda_k = 10$ and $\gamma_k = 50$. See Figure 2.

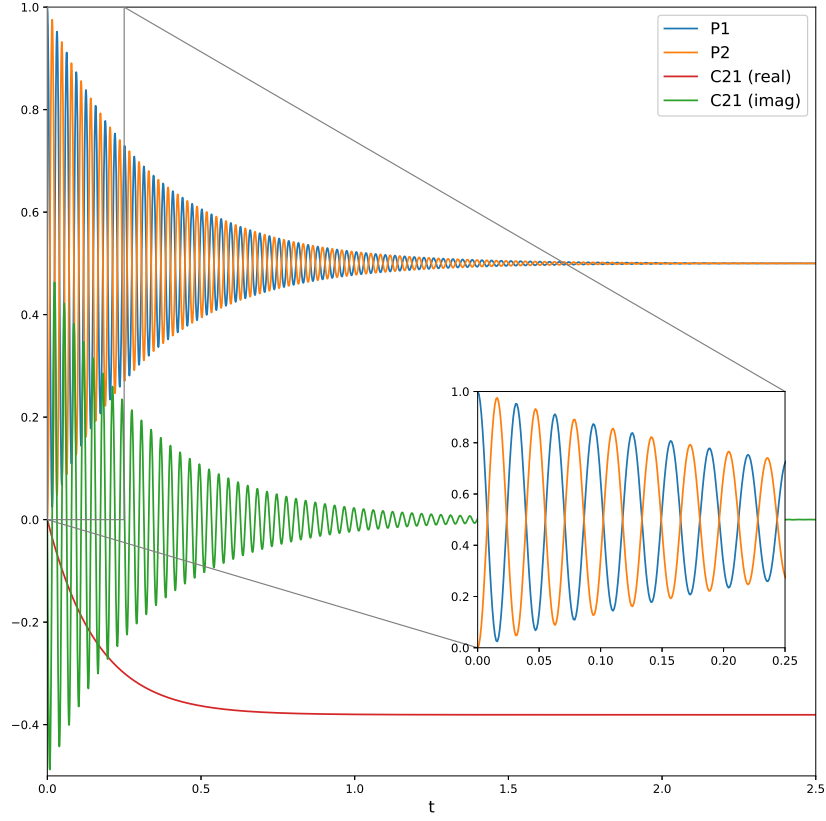


Figure 2: Obtained populations $P_1(t) = \langle 1 | \rho_s(t) | 1 \rangle$ and $P_2(t) = \langle 2 | \rho_s(t) | 2 \rangle$, and inter-site coherence $C_{21}(t) = \langle 2 | \rho_s(t) | 1 \rangle$, using Runge-Kutta method from $t = 0$ to $t = 2.5$. It can be seen that $P_1(t) = P_2(t) = 0.5$ for long enough times because of $\Omega_1 = \Omega_2$.

c) Same parameters from b) but now with $\Delta\Omega = \Omega_1 - \Omega_2 = 100$. See Figure 3.

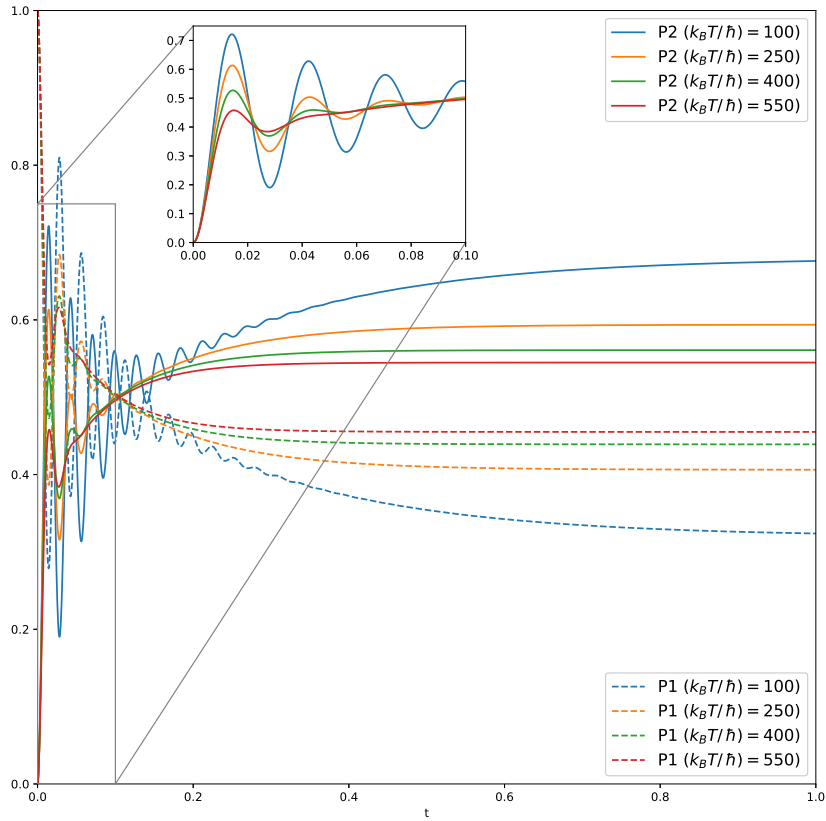


Figure 3: Populations $P_1(t) = \langle 1 | \rho_s(t) | 1 \rangle$ and $P_2(t) = \langle 2 | \rho_s(t) | 2 \rangle$ from $t = 0$ to $t = 1$. When saturated, $P_2^{(s)}$, becomes higher than $P_1^{(s)}$ because $\Omega_1 > \Omega_2$. This difference, $P_2^{(s)} - P_1^{(s)}$ is reduced when temperature increases.

d) The time evolution of the negativity of $\hat{\rho}_s(t)$ is simulated with the same parameters from **c)**, but now with a stronger environmental coupling $\lambda_k = 1000$. See Figure 4.

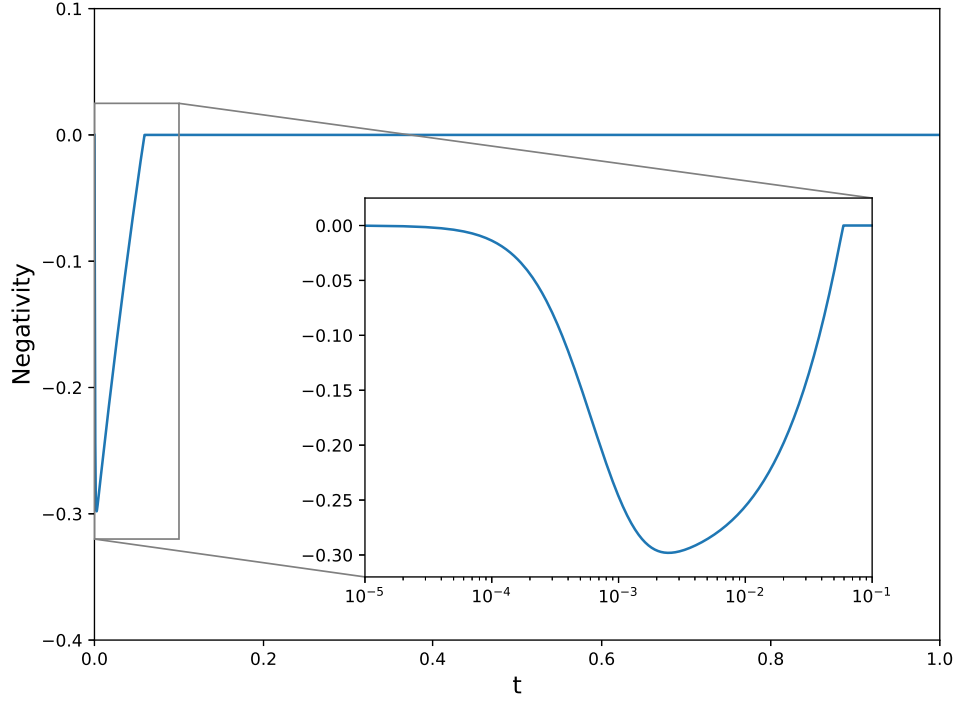


Figure 4: Negativity of $\hat{\rho}_s(t)$, i.e. the sum of its negative eigenvalues, from $t = 0$ to $t = 1$. A minimum of ≈ -0.3 is reached at $t \approx 2.5$ ms. After $t = 0.1$, the system $\hat{\rho}_s$ is positive semidefinite again.

e) With the same parameters from **d)**, the secular approximation is used to avoid the negativity. See Figures 5, 6 and 7

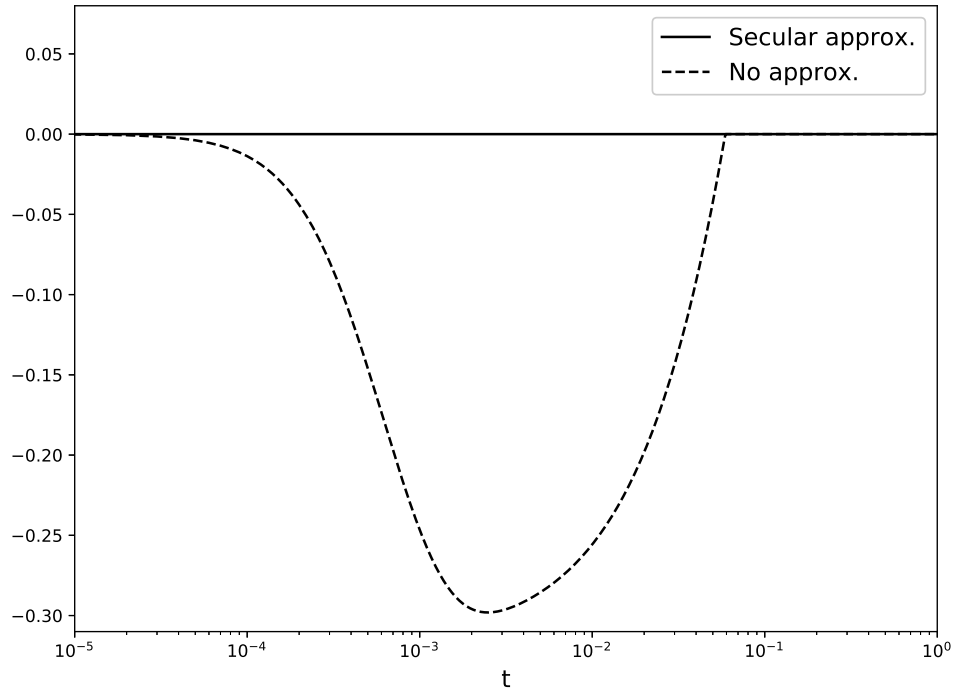


Figure 5: Negativity of $\hat{\rho}_s(t)$ from $t = 0$ to $t = 1$. When using the secular approximation (solid line) the negativity disappears.

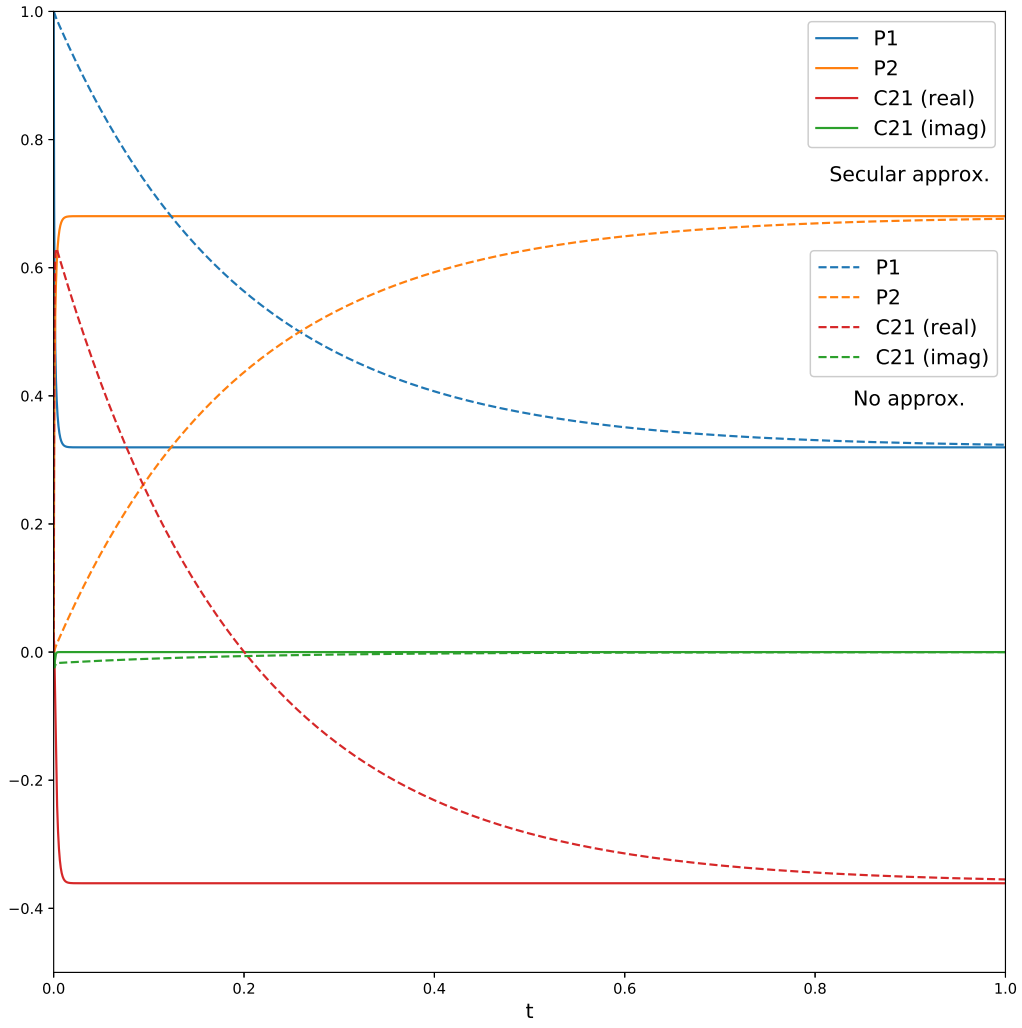


Figure 6: Time evolution of the populations and inter-site coherence using the secular approximation (solid lines) and without (dashed lines) from $t = 0$ to $t = 1$.

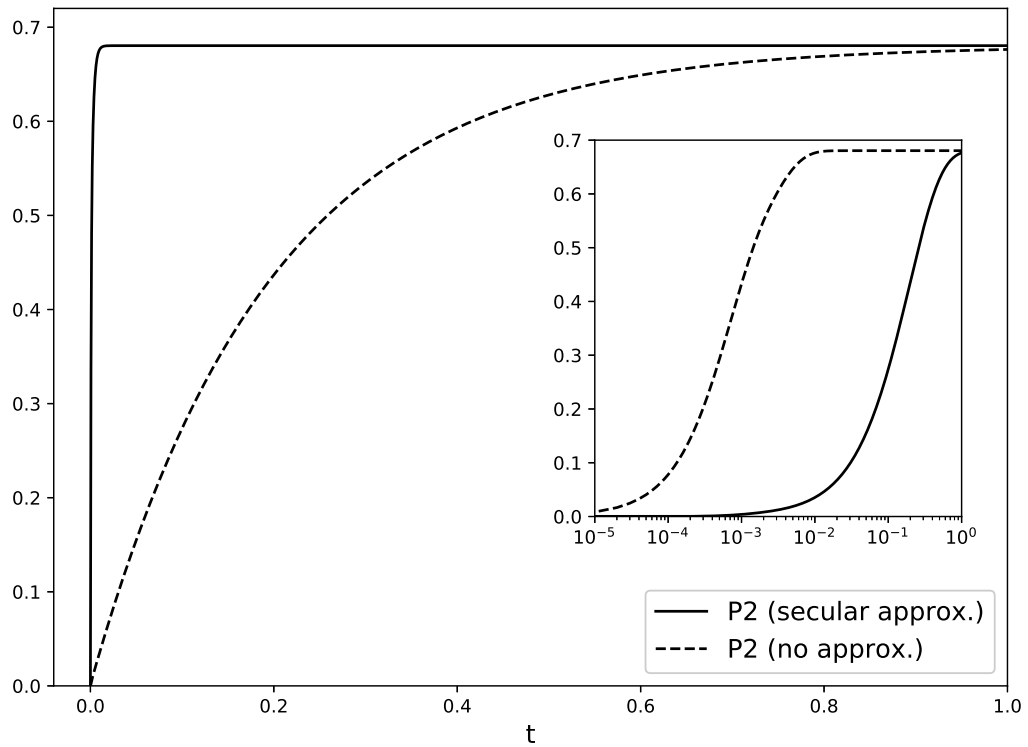


Figure 7: Time evolution of just the population of site 2 from $t = 0$ to $t = 1$.

f) For the last part, a moderate environmental coupling strength is considered ($J \approx \lambda_k$). This does not cause the negativity effect as before, but induces non-secular effects modulating system dynamics. See Figure 8.

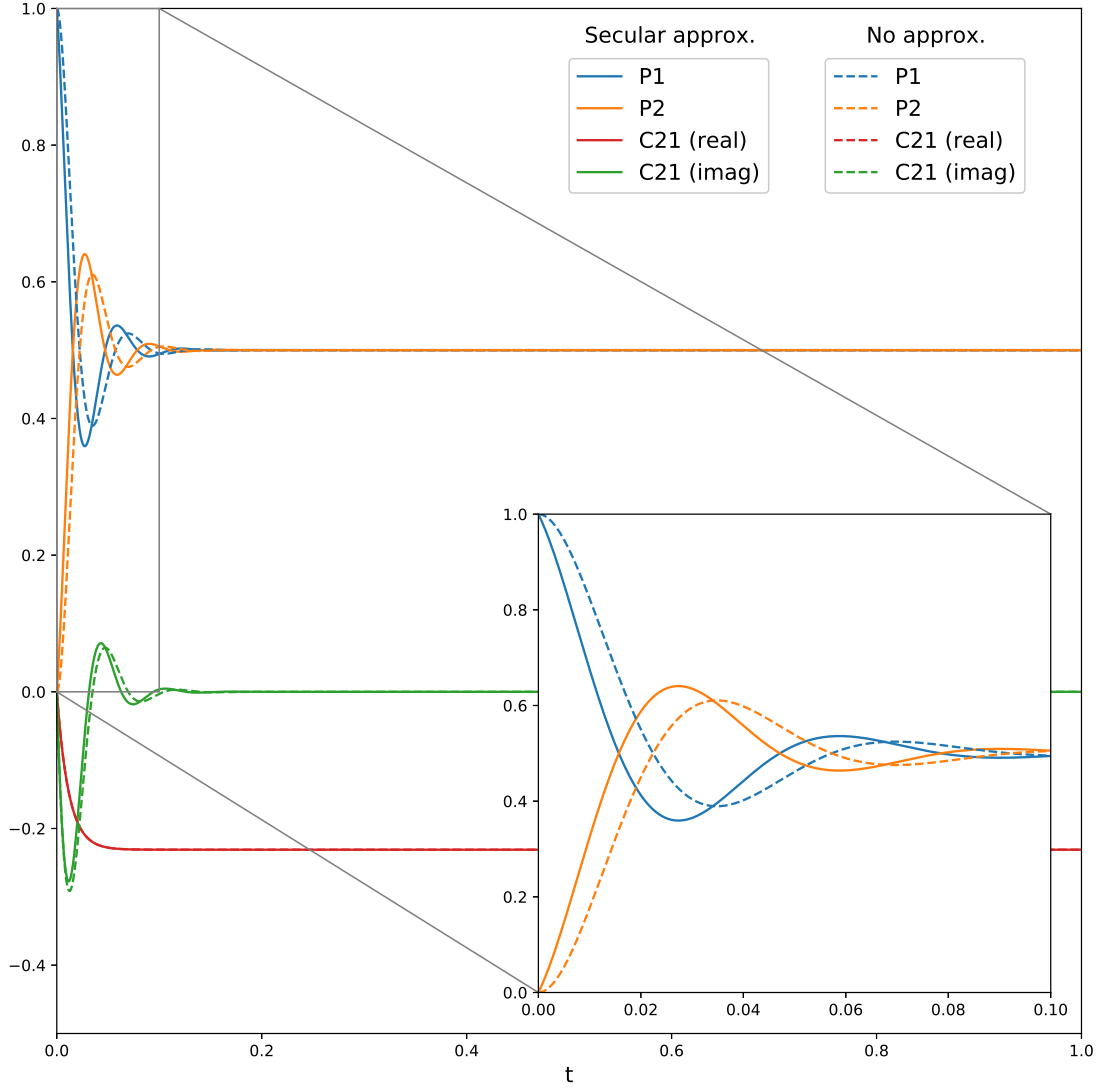


Figure 8: Time evolution of the site populations from $t = 0$ to $t = 1$. Non-secular effects can be observed before the saturation time ($t < 0.1$) in the zoomed area.